The effect of temperature and moisture on electrical resistance, strain sensitivity and crack sensitivity of steel fiber reinforced smart cement composite

2016 Smart Mater. Struct. 25 075024

(http://iopscience.iop.org/0964-1726/25/7/075024)

IOP Publishing Smart Materials and Structures
Smart Mater. Struct. **25** (2016) 075024 (10pp) doi:10.1088/0964-1726/25/7/075024

The effect of temperature and moisture on electrical resistance, strain sensitivity and crack sensitivity of steel fiber reinforced smart cement composite

Egemen Teomete

Dokuz Eylul University, Civil Engineering Department, Kaynaklar, Buca, Izmir, Turkey

E-mail: egemen.teomete@deu.edu.tr

Received 28 October 2015, revised 19 April 2016
Accepted for publication 10 May 2016
Published 10 June 2016

Abstract

Earthquakes, material degradations and other environmental factors necessitate structural health monitoring (SHM). Metal foil strain gages used for SHM have low durability and low sensitivity. These factors motivated researchers to work on cement based strain sensors. In this study, the effects of temperature and moisture on electrical resistance, compressive and tensile strain gage factors (strain sensitivity) and crack sensitivity were determined for steel fiber reinforced cement based composite. A rapid increase of electrical resistance at 200 °C was observed due to damage occurring between cement paste, aggregates and steel fibers. The moisture—electrical resistance relationship was investigated. The specimens taken out of the cure were saturated with water and had a moisture content of 9.49%. The minimum electrical resistance was obtained at 9% moisture at which fiber–fiber and fiber–matrix contact was maximum and the water in micro voids was acting as an electrolyte, conducting electrons. The variation of compressive and tensile strain gage factors (strain sensitivities) and crack sensitivity were investigated by conducting compression, split tensile and notched bending tests with different moisture contents. The highest gage factor for the compression test was obtained at optimal moisture content, at which electrical resistance was minimum. The tensile strain gage factor for split tensile test and crack sensitivity increased by decreasing moisture content. The mechanisms between moisture content, electrical resistance, gage factors and crack sensitivity were elucidated. The relations of moisture content with electrical resistance, gage factors and crack sensitivities have been presented for the first time in this study for steel fiber reinforced cement based composites. The results are important for the development of self sensing cement based smart materials.

Keywords: strain sensitivity, crack sensitivity, electrical resistance, moisture, temperature, cement, smart material

(Some figures may appear in colour only in the online journal)

1. Introduction

Structures are challenged by earthquakes, material degradations and other environmental factors. Concrete infrastructures have material deterioration while 30% of bridges in the USA were found to be structurally deficient (Reza *et al* 2003). Metal foil strain gages which are used in structural health monitoring have low durability, short life time and lower sensitivity than self sensing cement based composites (Chung 2001).

Carbon fiber inclusion decreases electrical resistance while load affects electrical resistance (Fu and Chung 1997, Fu *et al* 1997, Chung 1998). Strain and crack length were found to be strongly correlated with electrical resistance

(Teomete and Erdem 2011, Teomete 2013, Teomete and Kocyigit 2013, Teomete 2014).

Electrical resistance of the cement based materials has been probed using two and four electrode methods. In the two electrode method, current supply and voltage measurement were conducted using the same electrodes while in the four electrode method, different pairs were used. The four electrode method was not affected by sample cross section and distance between electrodes (Chiarello and Zinno 2005, Han *et al* 2007). In this study, the four electrode method was used.

Perimetral and embedded electrode configurations were adopted in tests of cement based materials. Conductive plate or mesh was inserted in the material in the embedded electrode method while a conductive wire or paint was attached to the perimeter in the perimetral electrode configuration (Reza *et al* 2004, Li *et al* 2006, Chen and Liu 2008, Li *et al* 2008). Copper wire mesh was inserted in the material as electrode in this study.

Researchers worked on piezoresistive and piezoelectric properties and applications of cement based composites for strain and damage sensing. Han *et al* (2011) developed vehicle detection sensors using nickel particle reinforced cement composite.

Different carbon nanotube weight percents and water/cement ratio were tested for piezoresistive sensitivities of multi walled carbon nanotube (MWCNT) cement composites (Han *et al* 2012a). Electrical resistance of carboxyl MWNT/cement composites was affected by strain and polarization due to DC current (Han *et al* 2012b).

Strain sensitivity of carbon fiber and carbon black filled cement based mixes were determined under single and cyclic compressive load (Han and Ou 2007). Wireless monitoring of compressive strain was achieved by nickel powder reinforced cement (Han *et al* 2008). Compressive strain sensitivity of nickel powder reinforced cement based composites was determined (Han *et al* 2009). Tunneling effect theory was used to model piezoresistivity of carbon black reinforced cement based materials (Xiao *et al* 2010). Cement based strain sensors were tested in structural elements (Xiao *et al* 2011, Baeza *et al* 2013, Sun *et al* 2014).

Lead zirconate titanate (PZT) piezoceramic was used in smart aggregate which was embedded in concrete for testing the concrete as communication channel (Siu *et al* 2014a-b).

Vipulanandan and Mohammed (2015) used iron oxide nanoparticles to enhance the piezoresistive behavior and compressive strength of smart cement for oil well applications. Increase in compressive strength, modulus of elasticity and gage factor by addition of iron oxide nanoparticles into cement composite was reported.

2-2 cement/polymer-based piezoelectric composite was investigated for its dielectric, piezoelectric and electromechanical coupling properties. The composite can be used for civil engineering ultrasonic transducer applications (Dongyu *et al* 2015).

Cement based piezoelectric composites were developed for traffic monitoring; pressure induced by vehicles was detected accurately (Zhang *et al* 2015). Piezoceramic-included smart aggregates were used to detect cracks and leakage in concrete water pipes (Feng *et al* 2015). Smart aggregates having piezoceramic were used to detect bond slip between steel plates and concrete in beams (Qin *et al* 2015). Lead zirconate titanate (PZT)-based smart aggregate embedded in concrete was used to evaluate the micro-structural and rheological properties of concrete from the fluid phase (Saravanan *et al* 2015).

The specific resistance of carbon fiber reinforced concrete (CFRC) decreased with increase of temperature and humidity (Guan *et al* 2005). The water saturated carbon fiber reinforced cement based material under percolation threshold had a gage factor 12% lower with respect to room temperature drying while variability of gage factor with strain amplitude and history increased (Wen and Chung 2008). Carbon fiber reinforced normal and self consolidating concrete were tested between -10 to $20\,^{\circ}\mathrm{C}$ for electrical resistance. Inverse exponential relationship between resistivity and temperature, which follows the Arrhenius relationship, was determined (Chang *et al* 2013).

In this work, the effects of temperature and moisture on electrical resistance, compressive- tensile strain gage factors and crack sensitivity were determined for steel fiber reinforced cement based composite. Tests with isolated specimens, which were heated with open table heaters, revealed that damage at cement paste, aggregate and steel fiber interfaces increased the electrical resistance dramatically. The relation between the electrical resistance and moisture showed that the excess water covering fibers increased the electrical resistance. The minimum electrical resistance was obtained at an optimal moisture value at which the fiber–fiber and fiber–matrix contacts were maximum while water in micro voids was acting as electrolyte. The mechanism between moisture content and electrical resistance was revealed for the first time for steel fiber reinforced cement based composite. Specimens having different moisture contents were tested with compression, split tensile and notched bending tests. The mechanisms between moisture content and compressive strain gage factor, tensile strain gage factor and crack sensitivity were determined as novel results. The steel fiber reinforced cement based composite can be used as a fire alarm sensor, moisture sensor for harmful water and strain sensor with known response to temperature and moisture.

2. Materials and experimental methods

The cement based composite had, by mass, the ratio of sand/cement 100%; silica fume/cement 10%; water/cement 40%; super-plasticizer Sika ViscoCrete High Tech 30/cement 1%. Brass coated steel fiber, which had a length of 6 mm and diameter of 290 μm, was used at 1% by volume in the mix. The brass coating was for corrosion protection. Special 5 cm cube and $4 \times 4 \times 16$ mm molds were designed and manufactured in this study. The molds had 2 mm wide slots on either side for locating copper wire mesh electrodes as seen in figures 1(a)–(b). The mix was cast in the mold and the specimens were removed from the mold 24 h after casting. The specimens were cured at 100% moisture for 28 days.

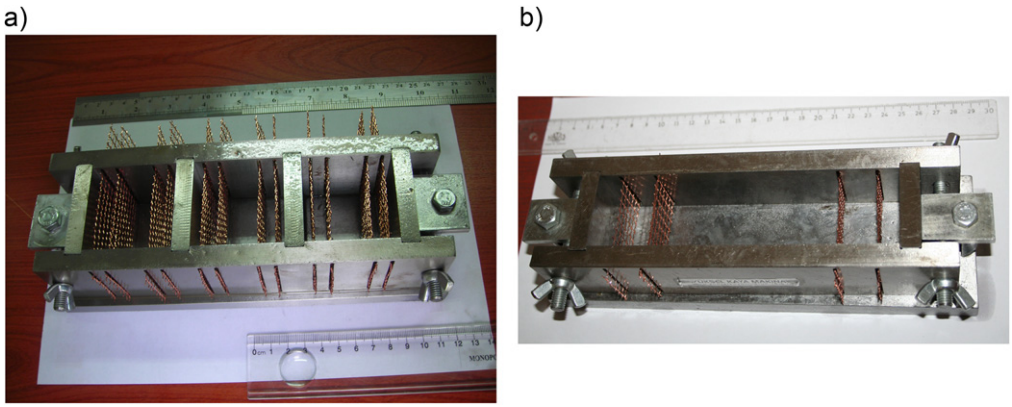

Figure 1. The special molds having 2 mm slots on either side for mesh electrode (a) 5 cm cube mold (b) 4 × 4 × 16 cm prism mold.

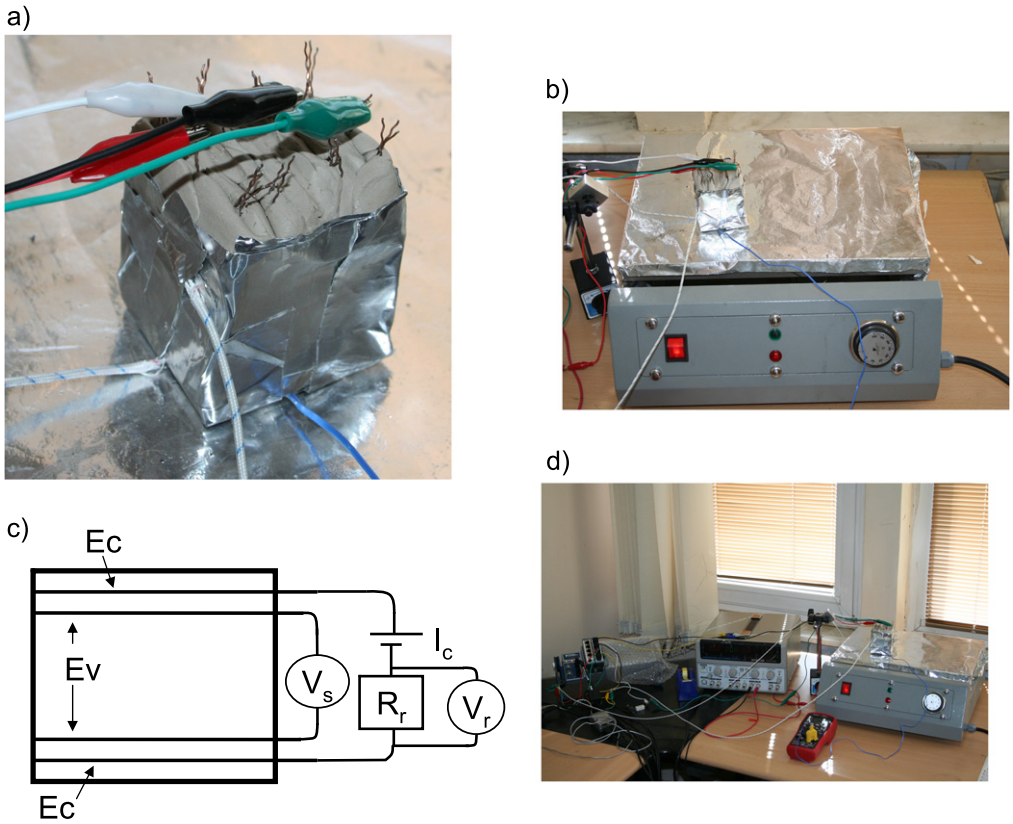

Figure 2. The temperature—electrical resistance test (a) the insulated sample (b) the sample on the heater (c) the test circuit (d) the equipment used.

2.1. Test of temperature effect on electrical resistance

Three 5 cm cube specimens were cast and cured. The specimens were left in laboratory atmosphere for 7 days to reach steady state moisture content. In order to test the specimens at constant moisture content at different temperatures, the specimens were coated with aluminum tape. Special ceramic clay was used to insulate the surface, which had electrodes coming out so that the electrodes did not short circuit as seen in figure 2(a). Thermocouples were attached on the bottom and top surfaces of the specimens to monitor the temperature. A specially designed and manufactured open table heater with a capacity up to 400 °C table temperature was used to heat the specimens as seen in figure 2(b).

The temperature of the heater's table was also monitored. The electric circuit used for the test is presented in figure 2(c). A DC power supply was used to feed the specimen and a reference resistance of $R_r = 1000$ Ohms was wired in series with the specimen. The current was supplied from the outer 2 electrodes of the specimen and the electrical potential was measured using the inner two electrodes as V_s. The electrical potential of the reference resistance was measured as V_r. The temperature of the specimen, V_s and V_r were measured using a National Instruments data logger. The equipment used at the

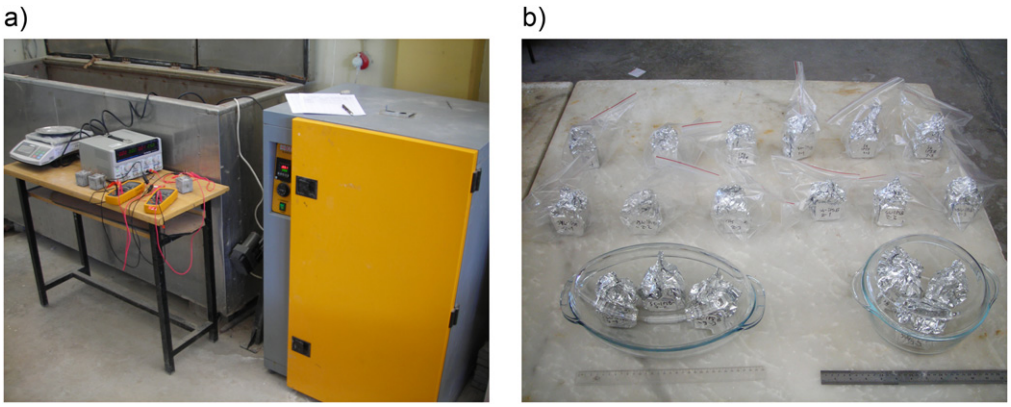

Figure 3. Test of moisture (a) equipments used (from left to right, weight, DC power supply, volt meters, furnace) (b) samples cooling in glassware and ready for mechanic tests.

test are presented in figure 2(d). NI cDAQ-9178 is an 8-slot chassis used for small, portable, mixed-measurement test systems. Eight different modules can be installed in the NI cDAQ-9178 chassis and simultaneously used. Modules can be used for measurements including voltage, current, thermocouples, RTDs, strain gages, load and pressure transducers, torque cells, accelerometers, flow meters, and microphones. The chassis is connected to PC via USB (www.ni.com).

NI 9219 module was used for temperature and voltage measurements. NI 9219 can be used with sensors such as strain gages, resistance temperature detectors (RTDs), thermocouples, load cells, and other powered sensors. The channels are individually selectable, so you can perform a different measurement type on each of the four channels (www.ni.com).

NI 9237 module was used for strain measurements in mechanical tests and contains all the signal conditioning required to power and measure up to four bridge-based sensors simultaneously. The NI 9237 can perform offset/null as well as shunt calibration and remote sensing, making the module suitable for strain and bridge measurements (www.ni.com).

At each point of the test, Ohm's law was used to determine the current in the circuit (I_c) and the specimen electrical resistance (R_s) as in equations (1), (2). The percent change in electrical resistance was determined using equation (3). R_{so} is the electrical resistance of the specimen at room temperature.

$$I_c = \frac{V_r}{R_r} \tag{1}$$

$$R_s = \frac{V_s}{I_c} \tag{2}$$

$$\%R = \left(\frac{R_s}{R_{so}} - 1\right) \times 100 \tag{3}$$

2.2. Test of moisture effect on electrical resistance

Three of 5 cm cube specimens were cast and cured as explained. Before and after heating at 90 °C for 10, 30, 60, 120, 210, 330 min, 20, 22.5, 28, 96.5, 145 h in a furnace, weight was measured and electrical resistance was determined using the circuit presented in figure 2(c) and equations (1)–(3). The test setup was presented in figure 3(a). The moisture content of the specimens was determined with respect to dry weight (W_{dry}) obtained at 145 h of 90 °C furnace time according to equation (4).

$$\text{Moisture}(\%) = \frac{(W - W_{dry})}{W_{dry}} \times 100 \tag{4}$$

In equation (4), W is the weight at a given furnace time, W_{dry} is the dry weight of the sample obtained at 145 hours of 90 °C furnace time.

2.3. Tests of moisture effect on strain sensitivity and crack length sensitivity

In order to determine the effect of moisture content on strain sensitivity (gage factor) for compression and split tensile tests, 30 cube specimens having dimension of 5 cm were cast and cured. 15 prism specimens which had dimensions of 4 × 4 × 16 cm were cast and cured to reveal the effect of moisture on crack length sensitivity. After 28 days of curing, the specimens were weighed and put in a furnace at 90 °C. At 30, 60, 120, 210, 330 min, three cube specimens for compression test, three cube specimens for split tensile test and three prism specimens (4 × 4 × 16 cm) for notched bending test were taken from the furnace, weighed and wrapped with aluminum foil to keep the moisture content constant. The specimens which were wrapped with aluminum foil were cooled in glassware and then kept in zip-lock bags until mechanical testing in order to keep the moisture content constant, as seen in figure 3(b).

Compression test was applied at a rate of 0.5 mm min^{-1} using a Shimadzu mechanical test machine. During the test, DC current was supplied from the outer two electrodes of the specimen while V_s was measured using the inner two electrodes as seen in figure 4(a). A reference resistance (R_r = 1000 Ohms) was used in series with the specimen and its potential difference was measured as V_r. A strain gage was

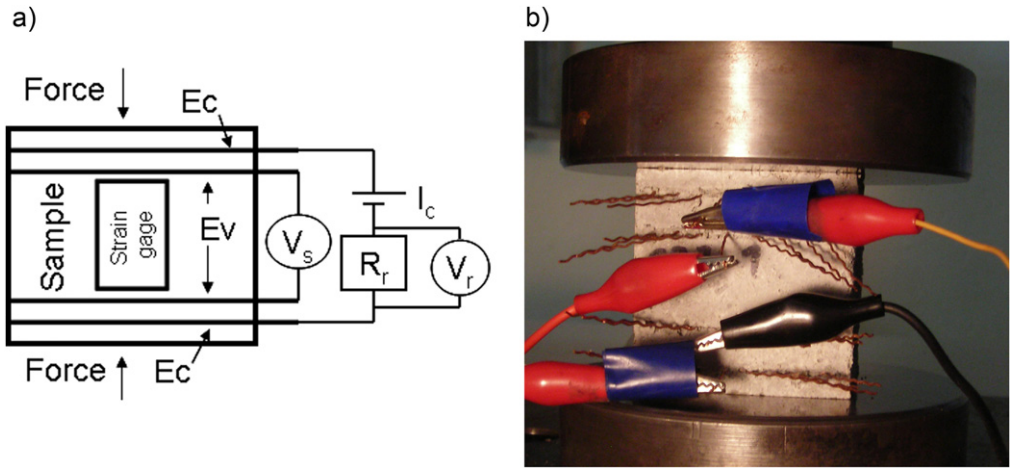

Figure 4. Compression test (a) electric circuit (b) sample at test.

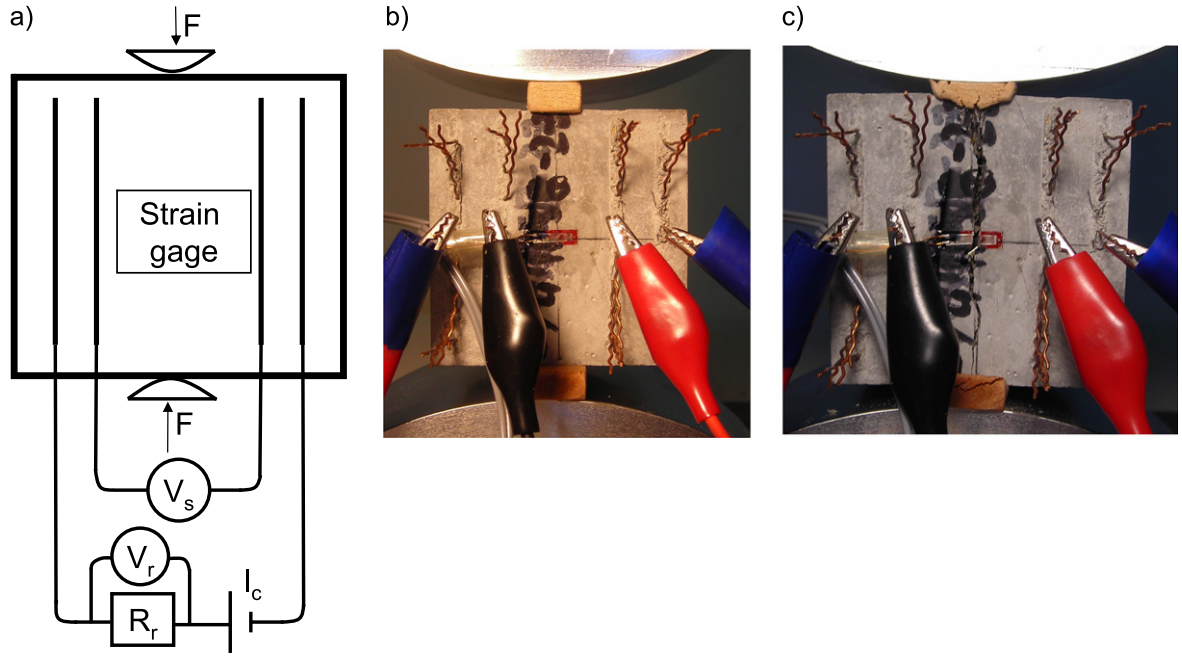

Figure 5. Split tensile test (a) circuit diagram (b) sample at test (c) sample after test.

used to monitor the strain of the specimen. V_s, V_r, and strain gage data were recorded at a rate of 10 Hz.

Split tensile test was conducted at a rate of 2.5 mm min^{-1} using Shimadzu mechanical test machine. Spherical loading plates conforming to EN 12390-6 (European Committee for Standardization 2009) were used at the test. Similar electric circuit as in compression test was used during the split tensile test as seen in figure 5(a). V_s, V_r, and strain gage data were recorded at a rate of 10 Hz. The specimen at test and after test is presented in figures 5(b), (c).

The notched bending test was conducted at a load rate of 0.2 mm min^{-1} by using a Shimadzu mechanical testing machine. The electric circuit, which was similar to the circuit used at compression test, is presented in figure 6(a). A notch was formed below the specimen by high speed electric cutter to control the crack growth. In order to monitor the real time crack length during the test, TML brand crack gages were attached above the notch on both sides of the specimens as seen in figure 6(b). The crack gage had grids each spaced with 0.5 mm. The crack propagation disrupts the conductive grids on the crack gage, changing its electrical resistance. V_s and V_r, and crack gage data were recorded at a rate of 10 Hz. The specimen after test is presented in figure 6(b).

The strain sensitivity is defined as gage factor (K) which is the fractional change in electrical resistance per unit strain as in equation (5).

$$K = \frac{(R_s - R_{so})/R_{so}}{\Delta\varepsilon} \tag{5}$$

In equation (5), Rs is the electrical resistance of the specimen at any time during the test, R_{s0} is the electrical resistance of the specimen without mechanical load, Δ_ε is the

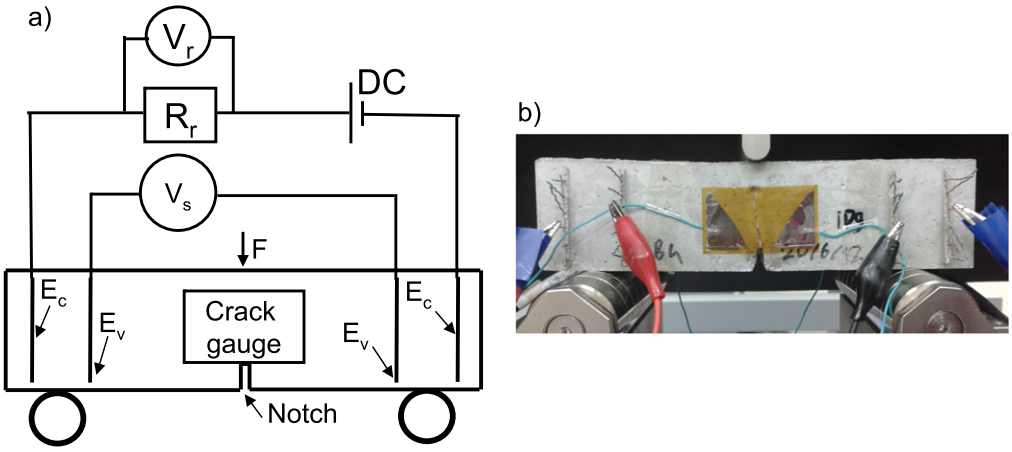

Figure 6. Notched bending test (a) Circuit diagram (b) Sample after test.

change in strain. Gage factor was determined for compression and split tensile tests.

For the notched bending test, crack sensitivity (*CS*) was defined as the percent change of electrical resistance per unit crack length in mm as in equation (6). The crack sensitivity is the slope of the *%R*–crack length curve. As the *CS* increases, the sensitivity of the cement composite for crack propagation increases. *CS* is a performance measure that can be used to develop damage sensors and damage sensing smart materials. *CS* has been first defined in this work for cement based composites.

$$CS = \frac{\%R}{L_{cr}} \tag{6}$$

In equation (6), *%R* is the electrical resistance change, L_{cr} is the crack length in mm.

3. Results and discussions

The experimental results and discussion are presented in this section.

3.1. Effect of temperature on electrical resistance

The cement based composite was isolated with aluminum tape and ceramic clay to prevent change of moisture content. The specimens were heated with an open table heater and electrical measurements were conducted simultaneously with temperature measurements. The change of electrical resistance with temperature is presented in figure 7(a). At room temperature, the electrical resistance was 351 Ohms. As the temperature increased up to 200 °C, the electrical resistance fluctuated and had a general trend of slight increase as seen in figure 7(b).

At 200 °C, the electrical resistance increased rapidly and at 243 °C, the electrical resistance passed over 39 000 Ohms (as seen in figure 7(a)). Neville (1996 pp 382) stated that the coefficient of thermal expansion of cement paste decreases above 150 °C and becomes negative above 200 °C, which means cement paste contracts above 200 °C. The reason of decrease of coefficient of thermal expansion of cement paste is the loss of water from hydrated cement paste and internal collapse. Mindess *et al* (2003 pp 461) named it 'structural break down of the hydration products'. Neville (1996 pp 382) and Mindess *et al* (2003 pp 461) stated that aggregate has a positive coefficient of thermal expansion at all temperatures; thus as the temperature increases the coefficient of thermal expansion of aggregates increases. Also, the steel fibers elongated by the increase of temperature. Thus, the reason of sudden increase in the electrical resistance above 200 °C and obtaining 39 000 Ohms at 243 °C was due to the contraction of cement paste while extension of aggregate and steel fibers. Tensile strain occurred in the cement paste, cement–aggregate and cement–steel fiber interfaces which developed damage; resulting in high electrical resistance of 39 000 Ohm.

3.2. Effect of moisture on electrical resistance

The moisture contents and electrical resistances of the specimens were monitored. The variations of the electrical resistance and electrical resistance change with respect to the moisture content are presented in figures 8(a), (b). As seen in figure 8(a), the moisture content of the specimens which were taken out from curing tank was 9.49%. As the moisture content decreased to 9%, the electrical resistance also decreased. The specimens taken from the cure were saturated with water. The steel fibers were coated with a thin film of water, which disrupts the fiber–fiber and matrix—fiber contacts. As the water content decreased, the fiber–fiber and fiber–matrix contacts increased leading to a decrease in electrical resistance. At the optimum moisture content of 9%, the fiber–fiber and fiber–matrix contact was maximum while the water in the micro voids acted as an electrolyte, conducting electrons, leading to the minimum electrical resistance. As the moisture dropped below 9%, the water in the micro voids which was acting as electrolyte decreased, leading to an increase in electrical resistance as seen in figure 8(a). The *%R*—moisture content relation had the same trend as presented in figure 8(b). The specimens reached the

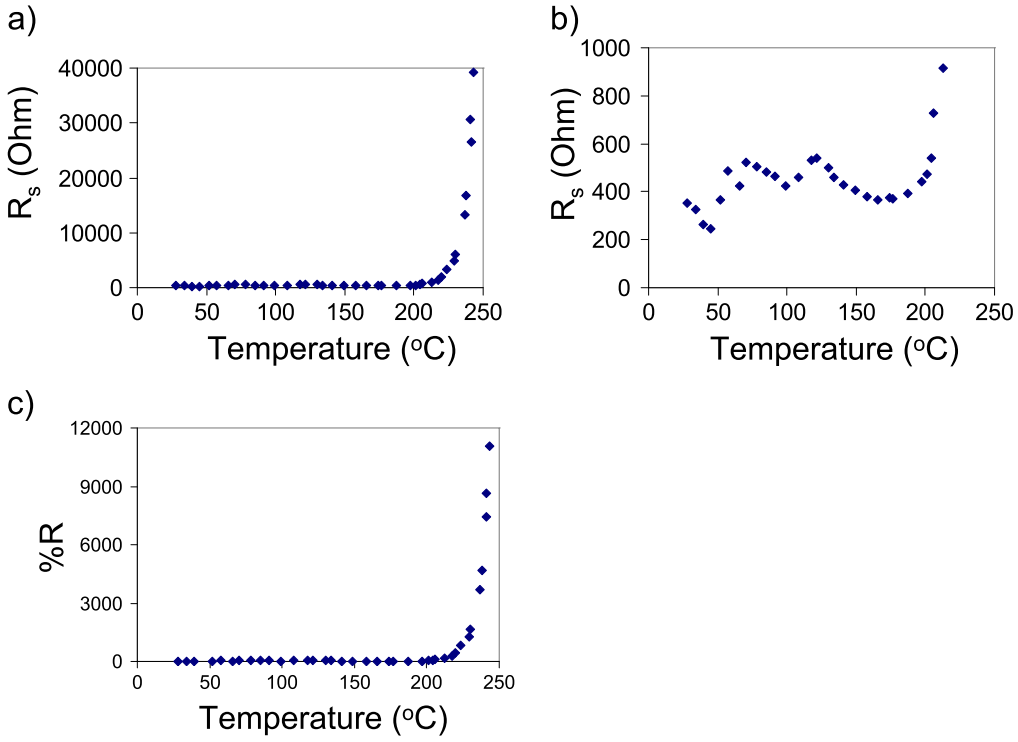

Figure 7. Variation of (a) electrical resistance with temperature (b) electrical resistance with temperature (magnified) (c) electrical resistance change with temperature.

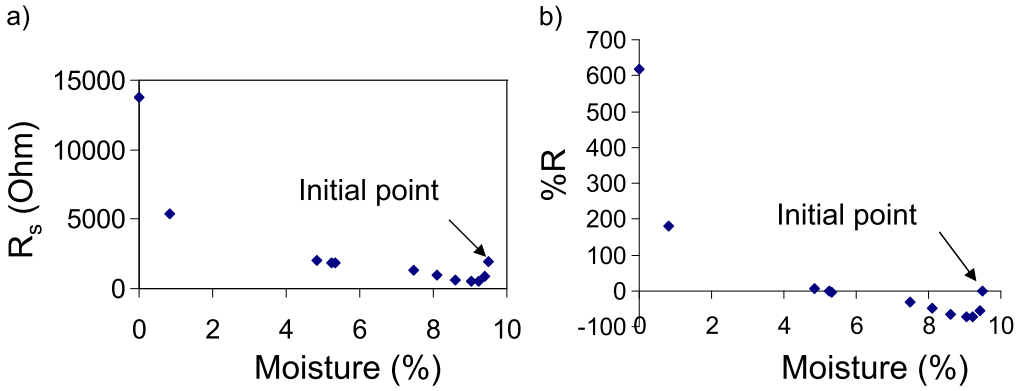

Figure 8. Variation of (a) electrical resistance with moisture (b) *%R* with moisture.

optimum moisture content of 9% at 60th minute in 90 °C . The same observations were obtained for all of the specimens.

3.3. Effect of moisture on strain sensitivity and crack length sensitivity

In order to determine the effect of moisture content on gage factor (strain sensitivity), three specimens were tested for each of 90 °C furnace time of 30-60-120-210-330 min with compression and split tensile tests.

The time histories of applied compressive strain, measured electrical resistance and variation of electrical resistance change (*%R*) with compressive strain were presented in figures 9(a)–(c) respectively. There is a strong linear relationship between the compressive strain and *%R* with a correlation coefficient of 0.97 as seen in figure 9(c).

The gage factor at compression test was maximum for the specimens which were left in 90 °C for 60 min as seen in figure 10(a). Above 60 min of 90 °C furnace time, the compression test gage factor decreased. The 60 min of 90 °C furnace time was an optimal time to attain the minimum electrical resistance at 9% moisture content. During compression test, the minimum electrical resistance was forced to decrease by increasing fiber–fiber and fiber–matrix contact which led to the maximum gage factor (strain sensitivity) for compression test as shown in figure 10(a).

The gage factor obtained for split tensile test increased by increasing 90 °C furnace time (decreasing moisture content) as seen in figure 10(b). As the moisture content decreased, the electrolyte water amount decreased; the role of fiber–fiber and matrix—fiber contacts increased in

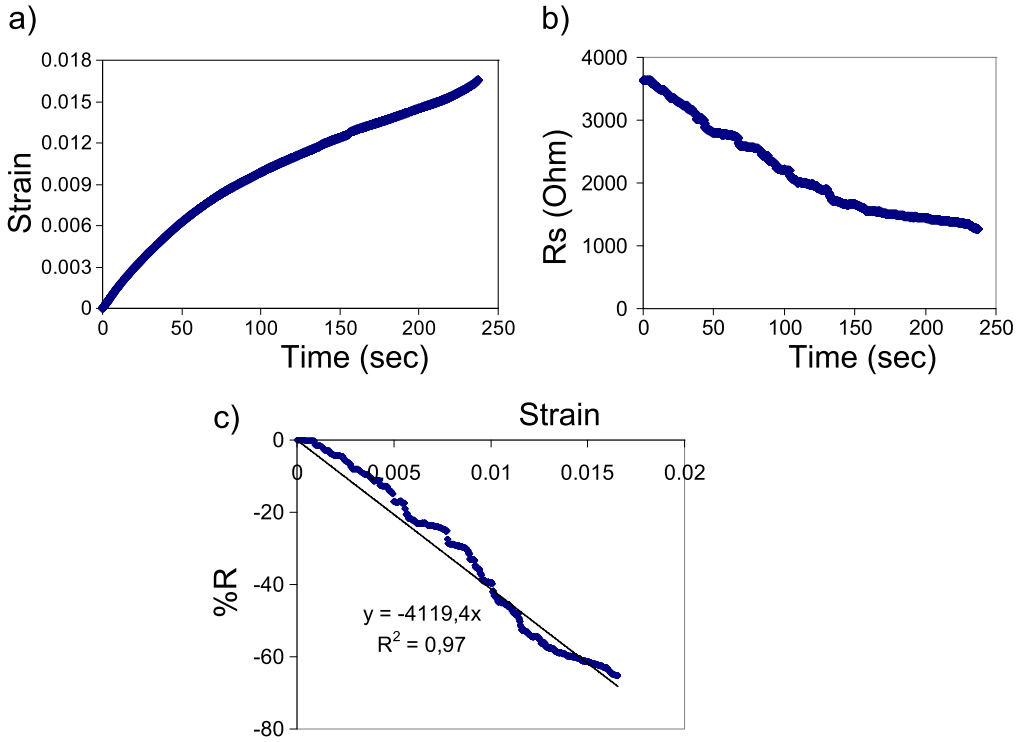

Figure 9. Compression test (a) strain—time (b) electrical resistance—time (c) electrical resistance change—strain graphs.

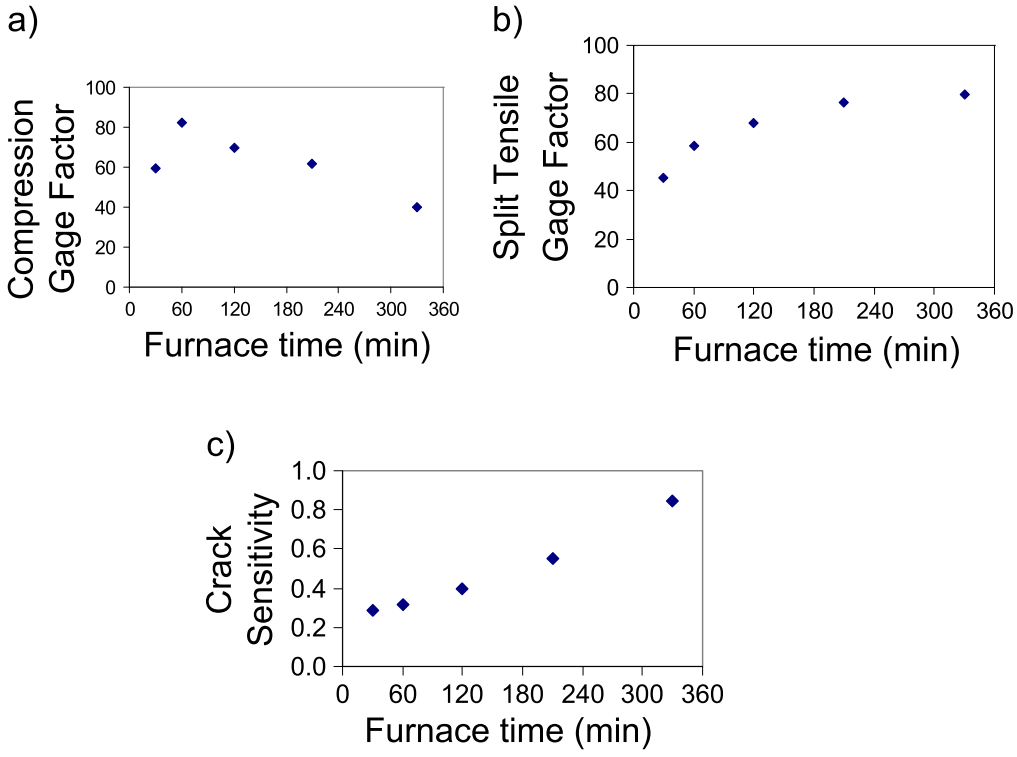

Figure 10. Variation of (a) compression test gage factor with 90 °C furnace time (b) split tensile test gage factor with 90 °C furnace time (c) crack sensitivity with 90 °C furnace time. Moisture content is inversely proportional to furnace time.

electron transfer. The tensile strain disrupts these contacts, leading to the increase in gage factor for split tensile test as seen in figure 10(b).

Similar results of split tensile testing were observed for the notched bending test for crack sensitivity–moisture content relationship. The decrease of the moisture content increased the role of fiber–fiber and fiber–matrix contacts. The crack propagation disrupted these contacts, leading to dramatic increase in electrical resistance, which caused the increase in crack sensitivity as seen in figure 10(c).

These results are important for development of cement based sensors and cement based smart materials.

4. Conclusions

The effects of temperature and moisture on the electrical resistance, strain sensitivity (gage factor for compression and split tensile tests) and crack sensitivity were determined experimentally for steel fiber reinforced cement based composite. Important results which can be used in smart materials and cement based sensors research are presented below:

1. The 5 cm cube specimens were isolated with aluminum tape to keep the moisture content constant. The specimens were heated with an open table heater while temperature and electrical resistance were measured simultaneously. After 200 °C mismatch strain between cement paste–aggregate and steel fibers developed damage which resulted in a rapid increase in the electrical resistance.
2. The change of electrical resistance with temperature makes the steel fiber reinforced cement based composite suitable for use as a fire alarm detector.
3. Five cm cube specimens were heated in the furnace at 90 °C. The moisture contents and electrical resistances were measured. The saturated specimens which were removed from cure had a moisture content of 9.49%. The electrical resistance decreased by decreasing moisture content from 9.49% to 9%. Above 9% moisture content, the fibers were coated with a thin film of water which disrupted fiber–fiber and fiber–matrix contacts. As the moisture decreased from 9.49% to 9%, the fiber–fiber and fiber–matrix contacts increased, leading to a decrease in the electrical resistance. The fiber–fiber and fiber–matrix contact was maximum while the water in the micro voids acted as electrolyte, conducting electrons, leading to the minimum electrical resistance at optimum moisture content of 9%.
4. As moisture content decreased below the optimum value of 9%, the loss of water acting as electrolyte in micro voids increased the electrical resistance.
5. The change of electrical resistance with moisture enables the use of steel fiber reinforced cement based composite as a moisture sensor in foundations, piles, waste management pools, shore and off-shore structures exposed to harmful water, for moisture monitoring of concrete.

In order to assess the effects of moisture content on gage factors (strain sensitivities) of compression and split tensile tests, 5 cm cube specimens were tested with different moisture contents. The different moisture contents were achieved by heating the specimens at 90 °C for different amount of times. Also the effect of moisture content on crack sensitivity was determined with a similar process by applying notched bending tests. The results obtained are:

1. At optimal moisture content of 9% which led to the minimum electrical resistance, maximum gage factor (strain sensitivity) for compression test was obtained. The compressive strain forced to decrease the minimum electrical resistance, resulting in the highest strain sensitivity for compression test.
2. The decrease of moisture content decreased the electrolyte water while fiber–fiber and fiber–matrix contacts had an increasing role in electron transfer for increasing furnace time. The tensile strain in split tensile test disrupted these contacts and increased electrical resistance severely, increasing the gage factor for split tensile test (tensile strain sensitivity).
3. The role of fiber- fiber and fiber- matrix contacts increased in electron transfer by decreasing moisture content due to the loss of electrolyte water by increasing furnace time. The fiber- fiber and fiber- matrix contacts were disrupted by crack propagation which resulted in significant increase in electrical resistance. Thus, crack sensitivity increased by decreasing moisture content.
4. The mechanism leading to the increase in gage factor for split tensile test and crack sensitivity was similar, which was based on the dominancy of the fiber- fiber and fiber–matrix contacts as the electrolyte water was lost.

The performance and response of cement based materials for temperature and moisture changes are important in case of fire and different environmental conditions. The results presented in this work reveal the effects of temperature and moisture on steel fiber reinforced cement based material's electrical resistance, strain gage factors and crack sensitivities. The steel fiber reinforced cement based composite can be used as a temperature and moisture sensor, while its optimal moisture content is determined when it is used as a strain sensor. These results contribute to self sensing smart cement based materials research.

Acknowledgments

This work is supported by The Scientific and Technological Research Council of Turkey (TUBITAK) through Grant no: 110M221. The author would like to thank to Sika Construction Chemicals Co. for providing the silica fume and superplasticizer and to Bekaert Steel Fiber Co. for steel fibers used in this study. The author is thankful to Assoc. Prof. Dr Tahir Kemal Erdem for his contributions to the work.

References

Baeza F J, Galao O, Zornoza E and Garcés P 2013 Multifunctional cement composites strain and damage sensors applied on reinforced concrete (RC) structural elements *Materials* **6** 841–55

Chang C, Song G, Gao D and Mo Y L 2013 Temperature and mixing effects on electrical resistivity of carbon fiber enhanced concrete *Smart Mater. Struct.* **22** 035021

Chen B and Liu J 2008 Damage in carbon fiber—reinforced concrete, monitored by both electrical resistance measurement and acoustic emission analysis *Constr. and Build. Mater.* **22** 2196–201

Chiarello M and Zinno R 2005 Electrical conductivity of self-monitoring CFRC *Cem. and Concr. Comp.* **27** 463–9

Chung D D L 1998 Self-monitoring structural materials *Mater. Sci. Eng.* **22** 57–78

Chung D D L 2001 Review functional properties of cement—matrix composites *J. Mater. Sci.* **36** 1315–24

Dongyu X, Xin C, Banerjee S, Lei W and Shifeng H 2015 Dielectric, piezoelectric and damping properties of novel 2-2 piezoelectric composites *Smart Mater. Struct.* **24** 1–8

European Committee for Standardization 2009 EN 12390-6: testing hardened concrete—part 6. Tensile splitting strength of test specimens (www.en-standard.eu/csn-en-12390-6-testing-hardened-concrete-part-6-tensile-splitting-strength-of-test-specimens/?gclid=CKK3yPXr78wCFRFmGwodYEYFKA)

Feng Q, Kong Q, Huo L and Song G 2015 Crack detection and leakage monitoring on reinforced concrete pipe *Smart Mater. Struct.* **24** 1–8

Fu X and Chung D D L 1997 Effect of curing age on the self-monitoring behavior of carbon fiber reinforced mortar *Cem. and Concr. Res.* **27** 1313–8

Fu X, Ma E, Chung D D L and Anderson W A 1997 Self-monitoring in carbon fiber reinforced mortar by reactance measurement *Cem. and Concr. Res.* **27** 845–52

Guan X C, Han B, Tang M and Ou J P 2005 Temperature and humidity variation of specific resistance of carbon fiber reinforced cement *Proc. SPIE - Int. Soc. Opt. Eng. (San Diego, CA)* vol 5765(1-2) pp 1–7

Han B, Zhang K, Yu X, Kwon E and Ou J P 2011 Nickel particle based self-sensing pavement for vehicle detection *Measurement* **44** 1645–50

Han B, Guan X and Ou J 2007 Electrode design, measuring method and data acquisition system of carbon fiber cement paste piezoresistive sensors *Sens. and Actuators* A **135** 360–9

Han B, Han B Z and Ou J P 2009 Experimental study on use of nickel powder-filled Portland cement-based composite for fabrication of piezoresistive sensors with high sensitivity *Sens. and Actuators A- Phys.* **149** 51–5

Han B and Ou J P 2007 Embedded piezoresistive cement-based stress/strain sensor *Sens. and Actuators A- Phys.* **138** 294–8

Han B, Yu X, Kwon E and Ou J P 2012a Effects of CNT concentration level and water/cement ratio on the piezoresistivity of CNT/cement composites *J. of Comp. Mater.* **46** 19–25

Han B, Yu Y, Han B Z and Ou J P 2008 Development of a wireless stress/strain measurement system integrated with pressure-sensitive nickel powder-filled cement-based sensors *Sens. and Actuators A- Phys.* **147** 536–43

Han B, Zhang K, Yu X, Kwon E and Ou J P 2012b Electrical characteristics and pressure-sensitive response measurements of carboxyl MWNT/cement composites *Cem. and Concr. Comp.* **34** 794–800

Li H, Xiao H and Ou J 2006 Effect of compressive strain on electrical resistivity of carbon black-filled cement –based composites *Cem. and Concr. Comp.* **28** 824–8

Li H, Xiao H and Ou J 2008 Electrical property of cement-based composites filled with carbon black under long-term wet and loading condition *Comp. Sci. and Tech.* **68** 2114–9

Mindess S, Young J F and Darwin D 2003 *Concrete* 2d edn (NJ: Prentice Hall)

Neville A M 1996 *Properties of Concrete* 4th edn (England: Longman)

Qin F, Kong Q, Li M, Mo Y L, Song G and Fan F 2015 Bond slip detection of steel plate and concrete beams using smart aggregates *Smart Mater. Struct.* **24** 1–13

Reza F, Baston G B, Yamamuro J A and Lee J S 2003 Resistance changes during compression of carbon fiber cement composites *J. Mater. Civil Eng.* **15** 476–83

Reza F, Yamamuro J A and Batson G B 2004 Electrical resistance change in compact tension specimens of carbon fiber cement composites *Cem. and Concr. Comp.* **26** 873–81

Saravanan T J, Balamonica K, Priya C B, Reddy A L and Gopalakrishnan N 2015 Comparative performance of various smart aggregates during strength gain and damage states of concrete *Smart Mater. Struct.* **24** 1–13

Siu S, Ji Q, Wu W, Song G and Ding Z 2014a Stress wave communication in concrete: I. Characterization of a smart aggregate based concrete channel *Smart Mater. Struct.* **23** 1–9

Siu S, Qing J, Wang K, Song G and Ding Z 2014b Stress wave communication in concrete: II. Evaluation of low voltage concretestress wave communications utilizing spectrally efficient modulation schemes with PZT transducers *Smart Mater. Struct.* **23** 1–7

Sun M, Liew R J Y, Zhang M H and Li W 2014 Development of cement-based strain sensor for health monitoring of ultra high strength concrete *Constr. and Build. Mater.* **65** 630–7

Teomete E 2013 Relations of crack length and electrical resistance for smart cement based composites *Cement Wapno Beton* **18** 329–34

Teomete E 2014 Transverse strain sensitivity of steel fiber reinforced cement composites tested by compression and split tensile tests *Constr. and Build. Mater.* **55** 136–45

Teomete E and Erdem T K 2011 Cement based strain sensor: a step to smart concrete *Cement Wapno Beton* **16** 78–91

Teomete E and Kocyigit O I 2013 Tensile strain sensitivity of steel fiber reinforced cement matrix composites tested by split tensile test *Constr. and Build. Mater.* **47** 962–8

Vipulanandan C and Mohammed A 2015 Smart cement modified with iron oxide nanoparticles to enhance the piezoresistive behavior and compressive strength for oil well applications *Smart Mater. Struct.* **24** 1–11

Wen S and Chung D D L 2008 Effect of moisture on piezoresistivity of carbon fiber-reinforced cement paste *ACI Mater. J.* **105** 274–80

Xiao H, Li H and Ou J P 2011 Strain sensing properties of cement-based sensors embedded at various stress zones in a bending concrete beam *Sens. and Actuators* A **167** 581–7

Xiao H G, Li H and Ou J P 2010 Modeling of piezoresistivity of carbon black filled cement-based composites under multi-axial strain *Sens. and Actuators A- Phys.* **160** 87–93

Zhang J, Lu Y, Lu Z, Liu C, Sun G and Li Z 2015 A new smart traffic monitoring method using embedded cement-based piezoelectric sensors *Smart Mater. Struct.* **24** 1–8